

## A NUMERICAL INVESTIGATION OF THE FULL 3D TURBULENT FLOW IN KAPLAN HYDRAULIC TURBINES

**Daniel BALINT**, PhD Assistant\*

Department of Hydraulic Machinery  
"Politehnica" University of Timisoara

**Sebastian MUNTEAN**, Senior Researcher  
Center of Advanced Research in Engineering  
Sciences

Romanian Academy - Timisoara Branch

\*Corresponding author: Bv Mihai Viteazul 1, 300222, Timisoara, Romania

Tel.: (+40) 256 403692, Fax: (+40) 256 403700, Email: balint@acad-tim.tm.edu.ro

**Romeo SUSAN-RESIGA**, Assoc. Prof.

Department of Hydraulic Machinery  
"Politehnica" University of Timisoara

**Ioan ANTON**, Prof., Member of Romanian  
Academy

Department of Hydraulic Machinery  
"Politehnica" University of Timisoara

### ABSTRACT

This paper presents a complete numerical methodology for computing the 3D turbulent flows in Kaplan turbines, methodology which can be easily used in the engineering research. Turbulent simulations for 3D geometries are used mainly for analyzing the energetic characteristics of flow behavior as a second step after the ideal flow simulations. Generally, the flow in the hydraulic turbines is three-dimensional and unsteady; therefore the boundary conditions imposed are significant for reducing the time of the computation and the hardware resources required. The domain of the computation extends from the inlet of the spiral casing to the outlet of the draft tube.

In order to reduce the computing time, the domain of investigation is decomposed in sub-domains and a guide vane-runner mixing interface boundary condition is used for obtaining a coupled numerical simulation. The velocity field together with the turbulence parameters is imposed on the inlet surface of each sub-domain, respectively the pressure field and the backflow turbulence parameters are imposed on the outlet surface of the sub-domains. In the mixing interface case, the solution is iteratively computed until continuous velocity and pressure fields are obtained. The whole methodology is applied in case of Kaplan turbines from the Iron Gates I powerplant at variable discharge.

### KEYWORDS

3D full Kaplan turbine, turbulent flows, Iron Gates I powerplant, mixing interface method

### NOMENCLATURE

$g$	[m/s <sup>2</sup> ]	gravity
$p$	[Pa]	static pressure
$z$	[m]	axial coordinate
$v$	[m/s]	velocity
$r$	[m]	radial coordinate
$B$	[m]	distributor height
$D$	[m]	runner diameter
$H$	[m]	turbine head
$E=gH$	[m <sup>2</sup> /s <sup>2</sup> ]	specific energy
$M$	[Nm]	shaft torque
$Q$	[m <sup>3</sup> /s]	discharge
$\eta$	[-]	efficiency
$\rho$	[kg/m <sup>3</sup> ]	water density
$\varphi = \frac{Q}{\pi\Omega\left(\frac{D}{2}\right)^3}$	[-]	discharge coefficient

$\Omega$	[rad/s]	angular velocity
$\Psi = \frac{2E}{\left(\Omega\frac{D}{2}\right)^2}$	[-]	head coefficient [1]

### Subscripts and Superscripts

$dt$	draft tube
$gv$	guide vanes
$m$	mechanical
$r$	radial direction
$run$	runner
$sc$	spiral casing
$sv$	stay vanes
$t$	theoretic
$u$	tangential direction

## 1. INTRODUCTION

For industrial cases the inviscid numerical computations are easy to be done because of the reduced time of the computation involved. It may be the case of designing a new blade for the rotating parts of the machine. The problem is represented by the uncertainty of the numerical results achieved when using inviscid flows comparing to the real flow obtained in a hydraulic circuit of a machine.

Energetic parameters of the hydraulic machinery have been increasing in last years of practice. Bigger design solutions with high energetic and cavitation characteristics are developed. For having this, the geometric parameters of the hydraulic machinery become significant. In many cases the mechanical elements of the machinery are well designed and their efficiencies can be easily adjusted. As a consequence, the hydraulic efficiency remains an opened problem for developing a better machine.

3D inviscid computations are involved for the first step of the design process when a large amount of technical and geometrical solutions are developed. The geometrical parameters of the blades are directly linked to the energetic and cavitation behavior. When high energetic cascade foils are employed for a particular configuration of a machine, the inviscid simulations may present problems regarding the accuracy of the results obtained. In these cases, the turbulent flow simulations can bring to the light the real information about the flow phenomena inside the machine. The inviscid numerical simulations can predict well the behaviour of the flow in the neighbourhood of the best efficiency operating point.

## 2. DOMAIN DECOMPOSITION

For a better understanding of the flow behavior in practice, the whole hydraulic circuit of the machine should be taken into study. For the case of a hydraulic turbine, all its elements should be investigated. The main problem is represented by the huge time of computation and hardware resources involved. The grid accuracy and the flow models become important regarding the results.

One method of splitting the whole turbine and to couple the bodies obtained is presented in this paper. The main advantage is to reduce the time of the computation when different operating points should be investigated.

The spiral casing and the stay vanes are taken together because the geometry is constant when the operating point changes. The particularity is given by the boundary conditions employed for transfer the flow field to the guide vanes. A single guide vane channel is computed coupled to the runner channel

using the mixing interface technique. Finally, the draft tube of the Kaplan turbine is computed.

### 2.1. Spiral casing and stay vanes

The spiral casing for Kaplan turbine presents a polygonal section and is represented below. The domain is made longer upstream for having a better accuracy of boundary condition.

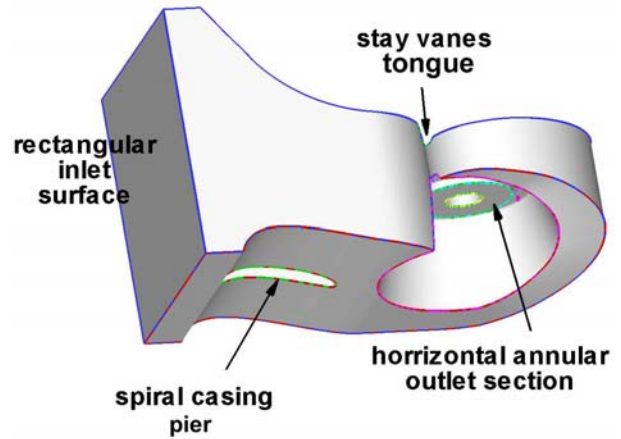


Figure 1. Domain of the computation used for the spiral casing of the Kaplan turbine of Iron Gates I

The stay vanes are placed inside the spiral casing domain and they are numbered clock-wisely starting from number 2 because the first one is represented by the tongue of the stay vanes (see Figure 2).

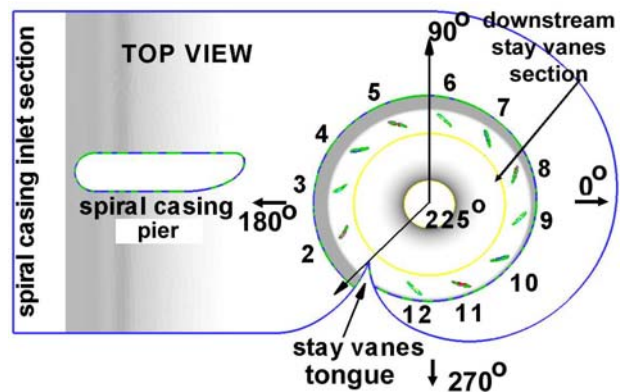


Figure 2. Stay vanes placement and indexes inside the spiral casing of the Kaplan turbine

The outlet section of the spiral casing and stay vanes domain is a horizontal plane upstream the runner blades. The total number of cells is of about 1.7 millions.

### 2.2. Guide vanes and runner

The computational time is reduced when only one interblade channel of the guide vanes and one channel of the runner are taken into account.

The Kaplan turbine of Iron Gates I powerplant consists of 32 symmetrical guide vanes and for the computation only one channel is used. The domain of the guide vane channel consists of about 220.000 structured cells.

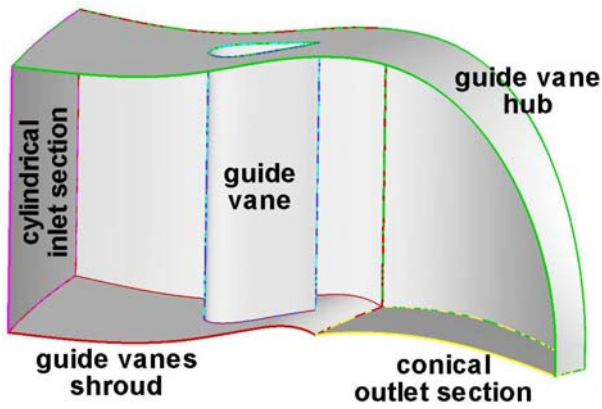


Figure 3. Guide vane domain of the Kaplan turbine

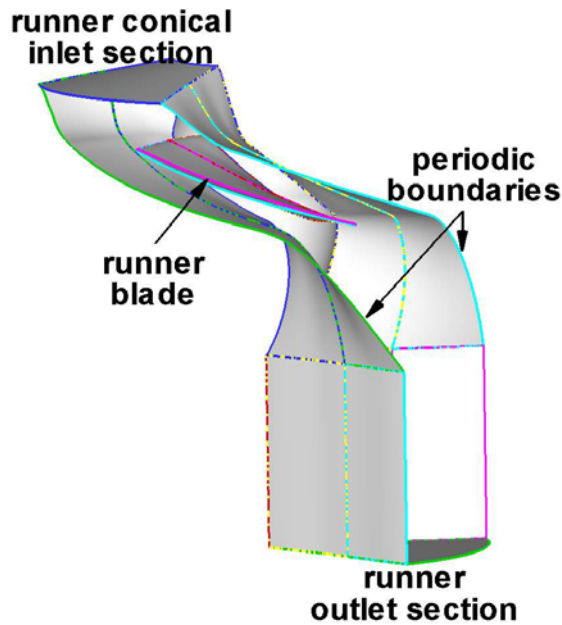


Figure 4. Runner periodic channel of the Kaplan turbine of Iron Gates I powerplant. Whole the runner domain is divided at the mean span for having a better mesh

The runner of the turbine has 6 blades and only one interblade channel is used for the numerical investigation. The total number of structured cells for the runner channel is of about 550.000.

The guide vane channel is extended upstream with a vertical cylindrical surface and the runner domain is extended downstream with a cylinder for having a well boundary condition imposing.

The distributor-runner interface is a conical surface with a slope of 10 degrees which may be powerful when using the mixing interface model. The mixing interface is employed successfully when there is no flow recirculation through it.

### 2.3. Draft tube

Draft tube of the Kaplan turbine is extended downstream with a cylinder for imposing the boundary condition on the outlet section [2].

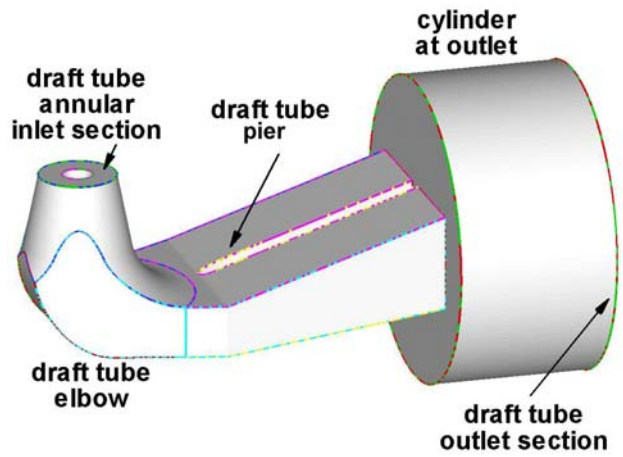


Figure 5. Draft tube domain of the Kaplan turbine

The inlet section of the draft tube domain is placed at the exit of the runner blade region which assures the complete swirling flow inside the draft tube at the end of the ogive of the runner hub.

The mesh of the draft tube consists of about 800.000 cells.

## 3. BOUNDARY CONDITIONS

### 3.1. Spiral casing and stay vanes

For the inlet surface of the spiral casing domain, the velocity field is imposed constant and normal on the surface. The velocity magnitude is computed using the discharge of the operating point.

On the outlet section, which is a horizontal plane as mentioned above, the pressure equilibrium is imposed:

$$\frac{\partial p}{\partial r} = \frac{\rho v_u^2}{r} \quad (1)$$

This pressure outlet boundary condition is used successfully in the case of small radial velocities and it is known that upstream the runner blades (as shown in Figure 1 the position of outlet section) the radial component of the velocity is small.

### 3.2. Guide vanes and runner

The velocity field obtained downstream the stay vanes (see Figure 2) are computed for the position of the inlet surface of the guide vanes (Figure 3).

Therefore, the radial velocity of the flow is computed for satisfying the flow rate of the operating point.

$$(v_r 2\pi r B)_{gvinlet} = (v_r 2\pi r B)_{sv downstream} \quad (2)$$

The tangential velocity of the flow is computed with respect to a constant circulation:

$$(rv_u)_{gvinlet} = (rv_u)_{sv downstream} \quad (3)$$

The axial velocity is neglected at the inlet section of guide vanes.

The guide vane channel and the runner channel are computed together using the mixing interface technique. First, the flow in guide vane domain is computed and after this the circumferentially averaged radial profile of the absolute velocity from the guide vane outlet section is imposed on the inlet section of the runner interblade channel. The flow in runner is solved and finally the circumferentially averaged radial profile of the static pressure from the runner inlet section is imposed on the distributor outlet section. The iterative process ends when a continuous flow is obtained through the distributor-runner interface [3] [4].

### 3.3. Draft tube

The radial profile of the velocity components downstream the runner blades, where the inlet surface of draft tube is placed as shown in Figure 5, is computed as an inlet velocity boundary condition for the draft tube.

The outflow boundary condition which assures no changing of the flow in normal direction is used for the outlet section of the draft tube. All domains of computation were developed in Gambit [5] and all the boundary conditions and the computations were made in Fluent commercial software [6].

## 4. TURBULENCE MODELS

The standard  $k-\varepsilon$  turbulence model was used for computing the flow in spiral casing, distributor and the runner [6]. Over all inlet and outlet (only for backflows) sections the turbulence intensity and length scale are imposed.

A turbulence intensity of 0.5% and a length scale of 0.005 m are imposed on the inlet of the spiral casing and the same values are used at the outlet section of the draft tube. The turbulence parameters obtained on the surface downstream the stay vanes are used for the inlet surface of the guide vanes. Also the turbulence parameters are computed iteratively on the distributor-runner interface. The turbulence obtained downstream the runner blade is imposed on the inlet surface of the draft tube.

The single surface where flow recirculations are encountered is the outlet of the draft tube, recirculations occurred for all the operating points involved. For draft tube domain the RNG  $k-\varepsilon$  turbulence model with swirl dominated flow was used. The wall boundary approach uses the enhanced wall treatment for all the walls.

The residuals of  $10^{-6}$  are used for all the domains as convergence criteria for the turbulent computations.

## 4.1. Solving strategies

First of all the steady inviscid numerical computations are completed for having a proper first guess of the flow inside the domains of the turbine.

For the spiral casing domain the standard  $k-\varepsilon$  model with default logarithmic wall functions are used after the inviscid computations. After the numerical solution is stabilized the enhanced wall boundary condition is imposed for all the walls.

Inviscid unsteady numerical computations are made for the draft tube domain after the steady inviscid process. This assures a good convergence of the numerical solutions for all the operating points employed.

The steady turbulent computations are made for obtaining an initialized turbulent flow field for the unsteady turbulent approach in the draft tube domain.

## 5. NUMERICAL RESULTS

The methodology presented above is applied for the case of Kaplan hydraulic turbines of Iron Gates I powerplant with a runner diameter of 9.5 m and a runner speed of 71.5 rpm.

Table 1. Parameters of the operating points taken for the numerical computation from the hill chart of the model of the Kaplan turbine of Iron Gates I before its refurbishment

Operating Point	Discharge $Q$ [m <sup>3</sup> ]	Head $H$ [m]
P085	438	31
P100	515	31
P115	592	31

Three operating points at constant head are used for the study. The discharge of the turbine is chosen at  $\pm 15\%$  of the discharge corresponding to the best efficiency operating point called P100.

## 6. STAY VANES OF THE KAPLAN TURBINE

One goal of the stay vanes shown in Figure 2 is to assure the mechanical strength of the spiral casing domain without being loaded by the flow.

In the above plot, the difference between the stay vanes loading when using inviscid and turbulent viscous models is shown.

From the stay vane number 5 to stay vane number 12 the difference between the two approaches is negligible for all the operating points discussed here. The explanation is that the flow is well adapted to the stay vanes.

The stay vanes indexes 2, 3 and 4 presents differences up to 20% for all the operating points involved. The chord length and the thickness of the stay vanes are

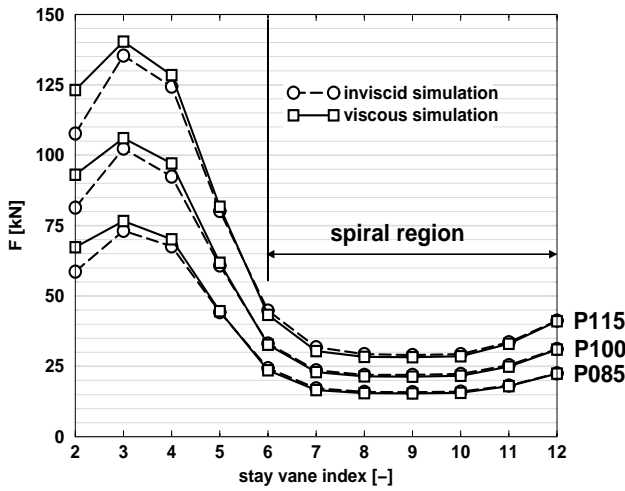


Figure 6. Force magnitude on the stay vanes of Kaplan turbines of Iron Gates I powerplant

smaller for these stay vanes and therefore the mechanical problems become significant.

The cause of such a high force magnitude on the stay vanes 2 to 5 is represented by the angle of incidence. The stay vanes are usually designed for having the camber curve aligned to the incident flow at leading edge and also for having the opening angle of the guide vanes regarding the designed operating point. In accordance to this, the curvature of the stay vanes increases up to values that may produce important hydraulic losses.

The high values of the mechanical strength found for these stay vanes are the effect of the spiral casing design and a possibility of reducing this effect is to adjust the geometry of the spiral casing in the design stage of the turbine.

The inviscid simulations for the spiral casing may bring a smaller influence of the angle of spiral casing

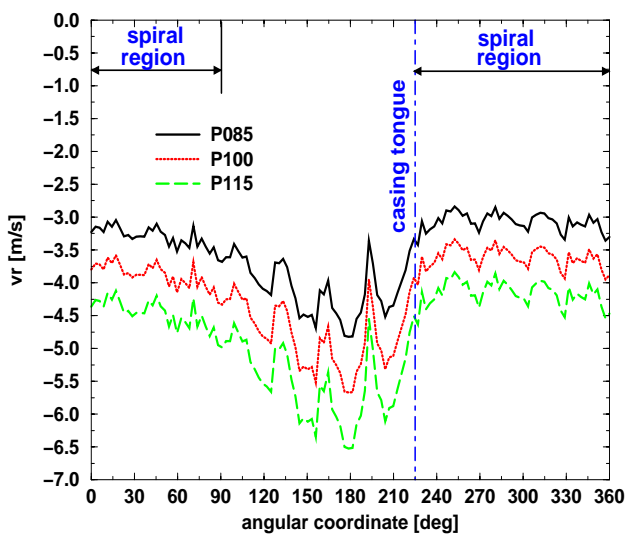


Figure 7. Radial velocity downstream the stay vanes of Kaplan turbine of Iron Gates I

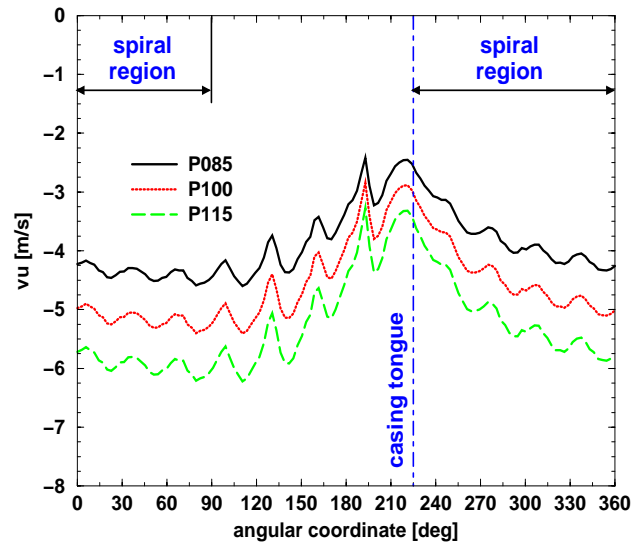


Figure 8. Tangential velocity downstream the stay vanes of the turbine

or the variation function of the transversal section versus the angular coordinate on a cylinder containing the axes of rotation of the guide vanes.

The radial velocity found for all the three operating points presents an increasing shape starting from angular position  $100^\circ$  until the position of stay vanes tongue. Is the position corresponding to stay vanes number  $2 \div 5$ .

On the other hand, the tangential velocity in this region decreases and therefore the flow is directly guided to the runner blades. A significant consequence of such a circumferential variation of the flow behavior is represented by the dynamic effects felt by the runner blades.

Even if the mean outflow angle is kept constant downstream the stay vanes when the flow discharge changes (see Table 2), the circumferential variation of the outflow angle can produce important vibrations of the runner.

Table 2. Outflow angle of stay vanes for variable discharge for Kaplan turbine

Operating Point	Mean outflow angle $\alpha^{\text{out}}$ [deg]
P085	42.873
P100	42.838
P115	42.840

The first mode amplitude is double than the second one for both radial and tangential velocities. This can be an element suitable for optimize the flow in the distributor of turbines. The 12nd mode amplitude represents the number of the stay vanes (including the tongue) and is unavoidable in the numerical computation process.

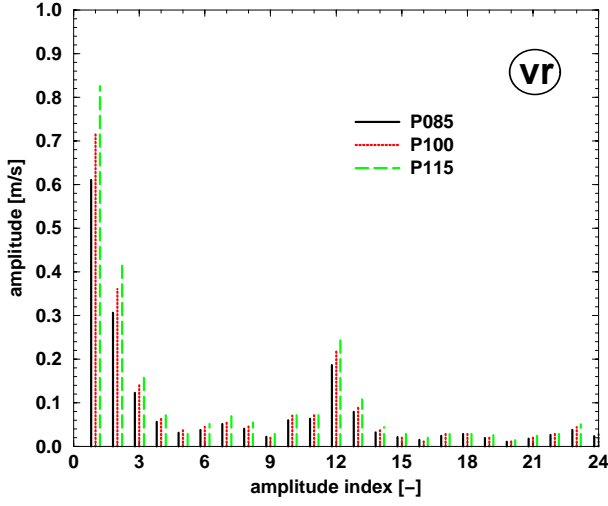


Figure 9. Mode amplitude for the Fourier representation of the radial velocity downstream the stay vanes

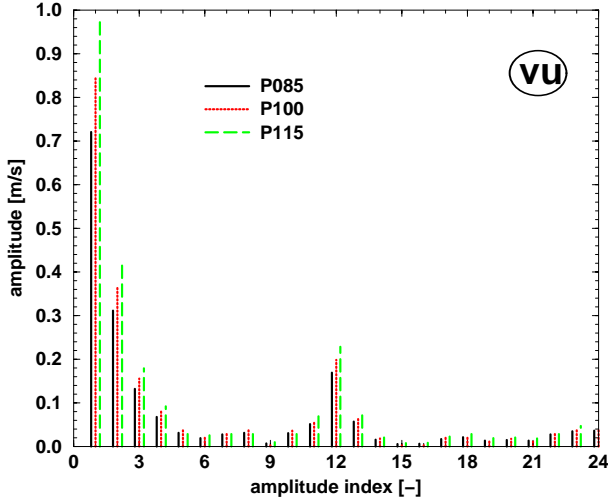


Figure 10. Mode amplitude for the Fourier representation of the tangential velocity downstream the stay vanes

### 7. 3D EFFECTS IN RUNNER DOMAIN

The difference occurred in the turbine practice comparing to the turbine design is still an opened subject. The neglecting of the radial motion of the flow is a common way to design the foil cascades of the Kaplan runner. Also the axial velocity is kept constant when the flow passes the runner cascades, in other words the curvature of the meridian channel is neglected.

These approximations accepted in the design process leads to 3D effects that are analyzed now.

A cause of the radial motion of the flow on the runner blade (see Figure 11) is the runner blade loading [7]. As a consequence the flow is pushed toward the shroud on pressure side of the blade and toward the hub on the suction side of the blade.

This 3D effect occurred in the runner domain leads to a different flow parameters regarding the ones accepted in the design process.

A possible method to increase the runner torque and efficiency is to use the radial motions of the flow by adjusting the stagger angle of the cascade foils of the runner blade and the blade axis position and shape (see also [8]).

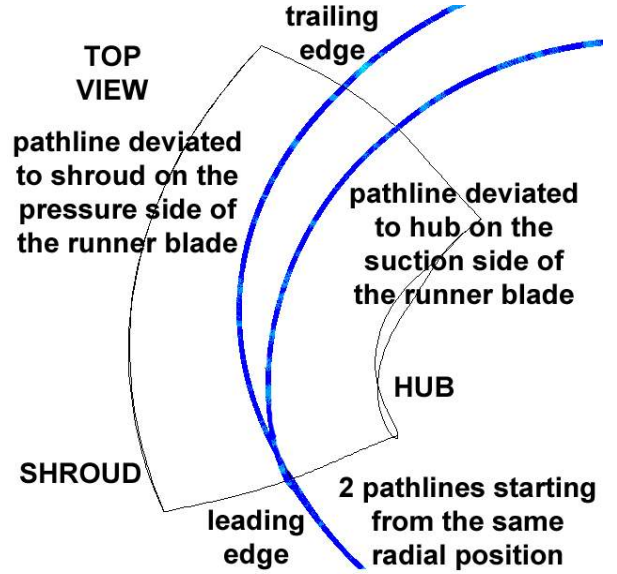


Figure 11. Flow deviation on the Kaplan runner blade due to blade loading

### 8. ENERGY AND EFFICIENCY

The energetic and cavitation behaviour of the turbines are in the interest of engineers. For this paper only energetic parameters are presented [9].

Available hydraulic specific energy is a sum of the energies of each turbine parts: spiral casing, stay vanes, guide vanes, runner and draft tube:

$$\Delta E_t = \Delta \left( p + \rho g z + \rho \frac{v^2}{2} \right) = \Delta E_{sc} + \Delta E_{sv} + \Delta E_{gv} + \Delta E_m + \Delta E_{run} + \Delta E_{dt} = \rho g H_t \quad (4)$$

The specific hydraulic energy on a particular surface  $S$  is computed as:

$$E_s = \frac{\iint_S \left( p + \rho g z + \rho \frac{v^2}{2} \right) (\vec{v} \cdot \vec{n}) dS}{\iint_S (\vec{v} \cdot \vec{n}) dS} \quad (5)$$

If whole the equation (4) is divided to the right term, the hydraulic losses in each domain are obtained. The turbine hydraulic efficiency is obtained using the mechanical term of the equation as follows:

$$\eta_t = \frac{\Delta E_m}{\rho g H_t} = \frac{\frac{M\Omega}{Q}}{\rho g H_t} \quad (6)$$

The torque  $M$  is computed as the momentum of the pressure and viscous forces on the pressure and suction sides of the runner blade.

The efficiency of each domain is computed using the hydraulic losses:

$$\eta = 1 - \frac{\Delta E}{\rho g H_t} \quad (7)$$

The hydraulic losses of the draft tube increase with the discharge because of the unsteady vortex generated from the ogive of the runner. Figure 15 shows that the vortex is splitted by the pier of the draft tube at the optimum operating point, but for the P115 operating point the vortex presents a large deviation to the left wall of the draft tube (see Figure 16).

In Figure 12 the distance between the efficiency curves represents the dimensionless hydraulic losses and it can be seen that the draft tube losses increase with the discharge as a consequence of the unsteady flow downstream the runner domain as presented in Figures 14÷16 for different discharge.

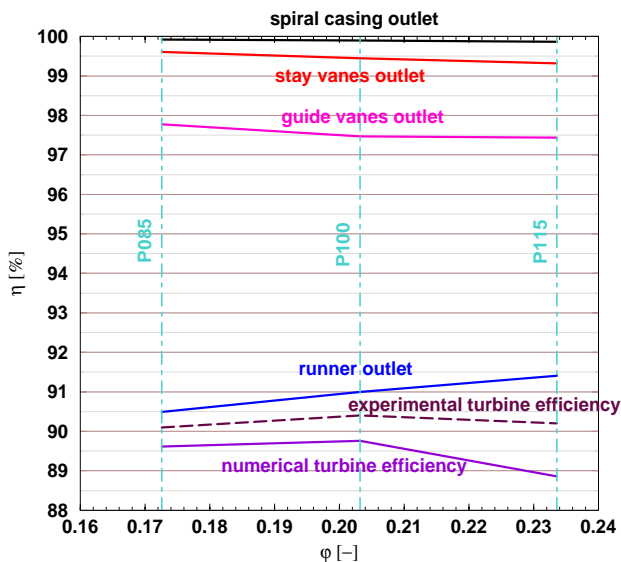


Figure 12. Turbine efficiency versus discharge coefficient for the complete Kaplan turbine [10]

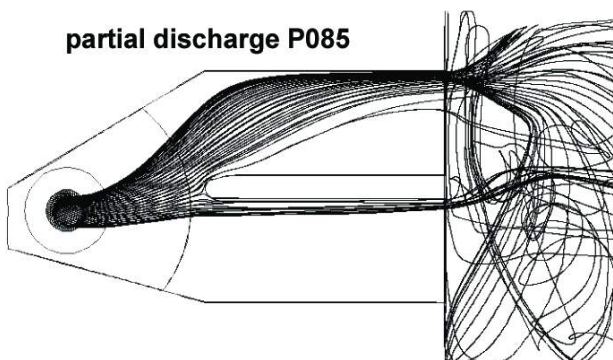


Figure 14. Streamlines starting from the ogive neighbourhood at partial discharge point P085

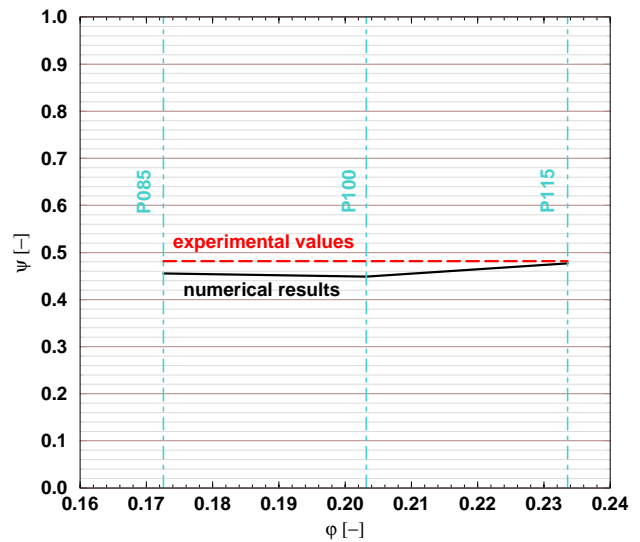


Figure 13. Head coefficient versus discharge one. The decreasing in efficiency at overloaded operating point P115 is felt by the head coefficient

**best efficiency point P100**

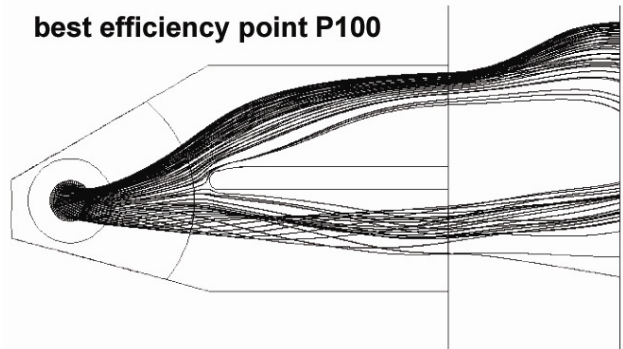


Figure 15. Streamlines starting from ogive neighbourhood at the best efficiency point P100

**overloaded operating point P115**

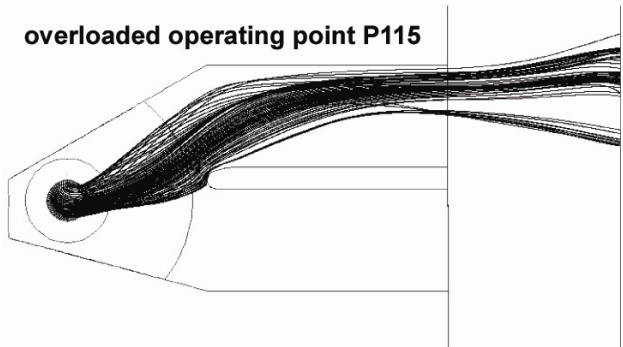


Figure 16. Streamlines starting from the ogive neighbourhood at overloaded operating point P115

## 9. CONCLUSIONS

The paper presents a 3D full turbulent numerical simulation performed for the case of Iron Gates I powerplant at variable discharge.

In the first part of the paper the domain decomposition for the Kaplan turbine and the boundary conditions used are described. The advantage of such

approach is represented by the reduced time of the computation that becomes important for industrial practice. Solving strategies employed are definitely significant for obtaining a stable numerical turbulent solution of the flow.

The difference obtained for the force on the stay vanes when using turbulent flows has shown that the differences occur when the incidence of the blade is not adapted to the hydraulic flow.

Also for these stay vanes, the flow downstream presents significant non-uniformities that are felt by the runner blade.

3D effects in the runner domain are described in section 7. These effects are generated by the runner blade loading and the meridian channel curvature over the blade design hypotheses.

The efficiency obtained for each turbine subdomain versus flow discharge shows the importance of the flow characteristics downstream the runner blades (see Figure 12). If the hydraulic losses are diminished in the runner, the ones in the draft tube are increased.

## ACKNOWLEDGMENTS

The present work has been supported from the National University Research Council Grant (CNCSIS) 109 / 2002, 109 / 2003 and 220 / 2004. Numerical computations have been performed at the Numerical Simulation and Parallel Computing Laboratory from the "Politehnica" University of Timisoara, National Center for Engineering of Systems with Complex Fluids.

## REFERENCES

1. International standard IEC (1999) No. 60193, Hydraulic turbines, storage pumps and pump-turbine - Model acceptance tests
2. Mauri S. (2002) Numerical simulation and flow analysis of an elbow diffuser. Ph.D. thesis, École Polytechnique Fédérale de Lausanne
3. Balint D., Resiga R., Muntean S. (2003) A numerical approach for the 3D flow in Kaplan turbines. Proceedings of the International Conference on CSHS03, Belgrade
4. Muntean S., Balint D., Resiga R., Anton I., Darzan C. (2004) 3D flow analysis in the spiral case and distributor of a Kaplan turbine, 22<sup>nd</sup> IAHR Symposium, Stockholm
5. Fluent Inc. (2001) Gambit 2. User's Guide, Fluent Incorporated, Lebanon
6. Fluent Inc. (2001) FLUENT 6. User's Guide, Fluent Incorporated, Lebanon
7. Vavra M. H. (1960) Aero-Thermo-dynamics and flow in turbomachines, John Wiley and Sons, Inc., New York
8. Brekke H. (2004) Design and operation of large turbines versus small hydro turbines, 22<sup>nd</sup> IAHR Symposium, Stockholm
9. Anton I. (2002) Energetic and cavitation scale-up effects in hydraulic turbines, Editura Orizonturi Universitare, Timisoara
10. Bartholomä K. (1997) Experimentelle und theoretische verlustanalyse in einer Kaplan vollspiral-turbine, Ph.D. Thesis, Technische Universität München